plicate laboratory photochemistry experiments including hydrocarbons. If the $2^2A''$ state is slightly bound at long O–O bond lengths, a temperature-dependent quantum yield for photolysis could be expected in the long-wavelength tail of the absorption band for this state.

Overall, the lower electronic states of methyl peroxy and resulting molecular properties are similar to those of HO_2, the simplest peroxy compound.

Supplementary Material Available: Detailed description of computational methods (4 pages). Ordering information is given on any current masthead page.

Structure, Bonding, and Dynamics in Heterocyclic Sulfur–Selenium Molecules, Se_xS_y

R. O. Jones* and D. Hohl

Contribution from the Institut für Festkörperforschung, Forschungszentrum Jülich, D-5170 Jülich, Federal Republic of Germany. *Received June 29, 1989*

Abstract: Density functional calculations have been performed for all crown-shaped cyclic isomers of the molecules Se_2S_6, Se_6S_2 (four each), and all cyclic trans isomers of Se_2S_5 and Se_5S_2 (twelve each). The incorporation of molecular dynamics with simulated annealing provides an efficient means for determining the geometries and relative energies and allows the study of structural rearrangements. Even in the low-symmetry molecules Se_xS_y, ground-state energies and the local structure of the energy surface can be determined accurately. The ground states in all molecules have (1,2)-structures, with adjacent minority atoms. In Se_2S_5 we observe a transformation at $T = 300$ K between vicinal (1,2)-conformers. Although the range of energies is very small in each molecule, the ordering of the different structures can be understood in terms of a simple model that allows predictions to be made for other group VIA heterocycles.

I. Introduction

Homocyclic molecules of sulfur (S_n) and selenium (Se_n) are among the best characterized of small atomic clusters. The group VIA elements are unique in that many allotropes comprise regular arrays of ring molecules, and X-ray structure analyses have been performed for S_n (n = 6–8, 10–13, 18, 20)[1,2] and Se_n (n = 6, 8).[1,3] It is natural that mixtures of sulfur and selenium have also received much attention, not only in the vapor phase[4,5] but also as liquids or as solid solutions.[6-8] Most samples prepared in the laboratory comprise a range of molecules, and the characterization of the crystalline phases obtained from the melts has been difficult. The different Se_xS_y species crystallize together, so that the crystal structures reported are disordered, with sulfur and selenium atoms distributed over the atomic sites.[9] The possible complexity is evident from the example of eight-membered rings, where 30 different crown-shaped isomers can occur.

Sulfur and selenium have much in common and it is not surprising that mixed isomers have similar energies and can coexist. The identification and structure of the molecular units in heterocyclic Se–S systems have been the subjects of continuing interest. Apart from the intrinsic interest in the molecules, an understanding of their structures should provide insight into the complex structures of related liquid and amorphous materials, including Se itself. Early kinetic work[4,5] on the molecules was interpreted to exclude the possibility of Se–Se bonds in S_nSe_{8-n} rings, and this was traced[4] to the fact that the Se–Se bond is weaker than both S–S and Se–S bonds. Raman spectroscopy has shown, however, that Se–Se stretching vibrations can readily be identified in such structures,[10] even for mixtures with very low Se concentrations. On the other hand, the S–S stretching band was not seen if the nominal sulfur content dropped below that in Se_6S_2, suggesting that the formation of S–S homonuclear bonds is not favored in mixed crystals with low sulfur content. This apparent asymmetry between S-rich and Se-rich molecules was also attributed to the relative weakness of Se–Se bonds.[10]

The last decade has seen considerable use of Raman spectroscopy to study these systems, with impressive results. The structures of the eight-membered systems 1,2,3-Se_3S_5[11] and 1,2,5,6-Se_4S_4[12] have been determined qualitatively, and the first rings with less than eight atoms [(1,2)-Se_2S_5 and SeS_5] have been prepared and characterized.[13] Ring molecules with a majority of Se atoms (Se_5S, Se_5S_2, Se_6S_2)[14] have also been studied. A comparison with Urey-Bradley force-field calculations of fundamental vibration frequencies of six- and seven-membered Se–S heterocycles[15] showed that the ground state of the last of these contained adjacent Se atoms. ^{77}Se NMR spectroscopy has been used recently[16] to identify isomers of Se_nS_{8-n} obtained from molten mixtures of the elements. The main components were found to be SeS_7 and (1,2)-Se_2S_6, with smaller amounts of twelve others. For a given chemical composition, isomers with all Se atoms adjacent to each other were the most abundant. In the case of Se_2S_5, the ^{77}Se NMR signal in CS_2 solution has a single peak at room temperature, so that the Se atoms are magnetically equivalent on the NMR time scale.[17] In Se_5S_2, the NMR spectrum shows that there are three sets of nonequivalent Se

(1) Donohue, J. *The Structures of the Elements*; Wiley: New York, 1974; Chapter 9.
(2) Steudel, R. In *Studies in Inorganic Chemistry*; Müller, A., Krebs, B., Eds.; Elsevier: Amsterdam, 1984; Vol. 5, p 3.
(3) Steudel, R.; Strauss, E. M. *Adv. Inorg. Chem. Radiochem.* **1984**, *28*, 135.
(4) Cooper, R.; Culka, J. V. *J. Inorg. Nucl. Chem.* **1967**, *29*, 1217.
(5) Schmidt, M.; Wilhelm, E. *Z. Naturforsch.* **1970**, *25B*, 1348.
(6) Steudel, R.; Laitinen, R. *Top. Curr. Chem.* **1982**, *102*, 177.
(7) Bitterer, H., Ed. *Selenium: Gmelin Handbuch der Anorganischen Chemie*, 8. Aufl., Ergänzungsband B2; Springer: Berlin, 1984.
(8) Steudel, R.; Strauss, E. M. In *The Chemistry of Inorganic Homo- and Heterocycles*; Academic: London, 1987; Vol. 2, p 769.
(9) Laitinen, R.; Niinistö, L.; Steudel, R. *Acta Chem. Scand. A* **1979**, *33*, 737.
(10) Eysel, H. H.; Sunder, S. *Inorg. Chem.* **1979**, *18*, 2626.
(11) Laitinen, R.; Rautenberg, N.; Steidel, J.; Steudel, R. *Z. Anorg. Allg. Chem.* **1982**, *486*, 116.
(12) Giolando, D. M.; Papavassiliou, M.; Pickardt, J.; Rauchfuss, T. B.; Steudel, R. *Inorg. Chem.* **1988**, *27*, 2596.
(13) Steudel, R.; Strauss, E. M. *Angew. Chem.* **1984**, *96*, 356.
(14) Steudel, R.; Papavassiliou, M.; Strauss, E. M.; Laitinen, R. *Angew. Chem.* **1986**, *98*, 81.
(15) Laitinen, R.; Steudel, R.; Strauss, E. M. *J. Chem. Soc. Dalton Trans.* **1985**, 1869.
(16) Laitinen, R. S.; Pakkanen, T. P. *Inorg. Chem.* **1987**, *26*, 2598.
(17) Steudel, R.; Papavassiliou, M.; Jensen, D.; Seppelt, K. *Z. Naturforsch.* **1988**, *43B*, 245.

0002-7863/90/1512-2590$02.50/0

atoms.[18] In both Se_2S_5 and Se_5S_2, the NMR spectra provide evidence for "pseudorotation", by which all ring atoms become equivalent within a certain time interval due to the simultaneous rotation about several of the ring bonds (see section III.C). The small energy barriers that this implies are consistent with the torsional barrier of S–S bonds in sulfur rings, which has been estimated from the heat of formation of S_7 to be $\leq$24 kJ mol^{-1}.[19]

Predictions of the relative stabilities of different isomers have been difficult to make. The interconversion of various Se_xS_y molecules and complicated ring–chain equilibration processes involve the rupture and formation of S–S, Se–Se, and Se–S bonds, and a theoretical study of reactions involving the groups

$$\text{–S–S–} + \text{–Se–Se–} \rightarrow 2\,\text{–Se–S–} \qquad (1)$$

has been performed recently with Hartree–Fock techniques with a minimal Gaussian basis.[20] Even with a single configuration and a restricted basis, the computing effort required for ab initio calculations of eight-membered rings was considered impracticable, and these authors restricted their attention to a number of hydrides containing these bonds. It was found that the energy changes of various rearrangement reactions related to (1) were very small (between 0 and –2 kJ mol^{-1}). The endothermic reaction is consistent with calorimetric measurements in the liquid [for an equimolar solution, the reaction enthalpy for (1) was concluded to be close to the enthalpy of mixing $\Delta H_m = +1.3$ kJ mol^{-1}].[21] For diatomic molecules in the gas phase,[22] the enthalpy change is $+7.9 \pm 6.7$ kJ mol^{-1} and the sum of the dissociation energies on the left side of (1) is greater than the sum on the right.

The stated uncertainties of energy differences in these calculations (10–20 kJ mol^{-1}) are, however, substantially greater than the energy differences themselves. Moreover, previous experience with other molecules containing group VIA elements has shown that the inclusion of effects beyond the HF approximation is essential.[23] The reliable prediction of the small energy differences in Se_xS_y molecules, with full geometry optimization and a thorough study of the convergence of the numerical technique, particularly the basis set, is a severe test of *any* method.

In this paper we present calculations of the ground-state geometries and relative energies of all isomers of the cyclic molecules Se_2S_6, Se_6S_2, Se_2S_5, and Se_5S_2. We use the density functional (DF) method,[24] with a local spin density (LSD) approximation for the exchange-correlation energy. This approach has given a remarkably good description of bonding trends in numerous families of molecules, including the group VIA molecules O_3, SO_2, and S_3.[23] Of particular relevance for the present work are the extensive calculations of ground-state geometries and relative energies for homocycles of both selenium (Se_n, $n = 3$–8)[25] and sulfur (S_n, $n = 2$–13).[26] The ground-state geometries found are in good agreement with structures determined by X-ray diffraction, and should be reliable predictions in cases where X-ray data are not yet available.

Essential for the success of these calculations has been the implementation of the combined molecular dynamics and density functional (MD/DF) approach suggested by Car and Parrinello.[27] The use of an LSD approximation avoids the uncertainties associated with parametrized energy surfaces, while the introduction of molecular dynamics is useful in two ways: First, the possibility of applying dynamical "simulated annealing" techniques means that one can avoid most of the numerous local minima on the potential energy surface. Second, MD allows us to study chemical dynamics and we have used it here to gain insight into the temporal and configurational evolution of a "pseudorotating" molecule (Se_2S_5). In the Se_n and S_n molecules investigated in our previous work,[25,26] the ground-state structures found did not depend on the starting geometries. Furthermore, the structure of the S_7O molecule[28] could be followed from a stable minimum in the ring structure across a high (5 eV) barrier to the experimentally known ground-state structure. The latter is an oxygen atom outside an S_7 ring and has an energy less than 0.2 eV below that of the ring minimum.

The method we use has been discussed in detail previously[26] and we describe in section II those aspects needed in the present work. In section III we present the results for the heterocyclic molecules. The discussion in section IV shows that the results can be understood in terms of a very simple picture that is readily transferable to other ring structures of the form Se_xS_y. We give our conclusions in section V.

II. Method of Calculation

The DF formalism shows that the ground-state properties of a system of electrons in an external field, V_{ext}, can be determined from a knowledge of the electron density, $n(r)$, alone. The ground-state total energy, E_{gs}, and density, n_{gs}, can be found by minimizing the relationship between energy and density, $E[n]$. It is convenient to write[29]

$$E[n] = T_0[n] + \int dr\, n(r)(V_{ext}(r) + \tfrac{1}{2}\Phi(r)) + E_{xc}[n] \qquad (2)$$

where T_0 is the kinetic energy of a system with density n in the absence of electron–electron interactions, $\Phi(r)$ is the Coulomb potential, and E_{xc} is the exchange-correlation energy. For the last term we adopt the LSD approximation

$$E_{xc}^{LSD} = \int dr\, n(r)\epsilon_{xc}[n_\uparrow(r),n_\downarrow(r)] \qquad (3)$$

Here $\epsilon_{xc}[n_\uparrow,n_\downarrow]$ is the exchange and correlation energy per particle of a homogeneous, spin-polarized electron gas with spin-up and spin-down densities $n_\uparrow$ and $n_\downarrow$, respectively. While different electron gas calculations lead to different values for ϵ_{xc}, and the same electron gas data can be parametrized in different ways, the consequences for calculated energy differences are not large. This is particularly true for equilibrium geometries. In the present work, we use the parametrization of Vosko et al.[30] of the electron gas data from quantum Monte Carlo calculations of Ceperley and Alder.[31]

The energy minimization is performed with standard MD techniques to follow the evolution of the system defined by the time-dependent Lagrangian[27]

$$\mathcal{L} = \sum_i \mu_i \int_\Omega dr |\dot{\psi}_i^*\dot{\psi}_i| + \sum_I \tfrac{1}{2} M_I \dot{\mathbf{R}}_I^2 - E[\{\psi_i\},\{\mathbf{R}_I\}] + \sum_{ij}\Lambda_{ij}\left(\int_\Omega dr\, \psi_i\psi_j^* - \delta_{ij}\right) \qquad (4)$$

Here M_I and R_I denote the ionic masses and coordinates, μ_i are fictitious "masses" associated with the electronic degrees of freedom, and the orthonormality of the single particle orbitals, $\psi_i(r,t)$, is guaranteed by the Lagrangian multipliers Λ_{ij}. From these orbitals and the resultant density $n(r,t) = \sum_i|\psi_i(r,t)|^2$, we use eq 2 to evaluate the total energy E in eq 4. The dynamics given by the Lagrangian $\mathcal{L}$ can be used to generate Born–Oppenheimer (BO) trajectories of the nuclei by an appropriate choice of the μ_i and initial conditions.

Periodic boundary conditions are used, and the large unit cell [constant volume 1000 Å^3; fcc lattice constant 15.9 Å] guarantees a very weak interaction between the clusters. The S and Se atoms are described by non-local pseudopotentials, using the angular momentum representation and the pseudopotential components for $v_l(r)$ ($l = 0$, 1, 2) of Bachelet et al.[32] The approximation used in earlier work ($v_{l\geq 2}(r) = v_1(r)$)[25,26] is not appropriate for Se for the high accuracy required to determine the

(18) Steudel, R.; Papavassiliou, M.; Krampe, W. *Polyhedron* **1988**, *7*, 581.
(19) Steudel, R. *Angew. Chem.* **1975**, *87*, 683; *Z.* Naturforsch. **1983**, *38B*, 543.
(20) Laitinen, R.; Pakkanen, T. *J. Mol. Struct. (Theochem)* **1983**, *91*, 337; **1985**, 124, 293.
(21) Maekawa, T.; Yokokawa, T.; Niwa, K. *Bull. Chem. Soc. Jpn.* **1973**, *46*, 761.
(22) Drowart, J.; Smoes, S. *J. Chem. Soc., Faraday Trans. II* **1977**, *73*, 1755. In line with these authors, we adopt the third-law value of the reaction enthalpy. The second-law value is somewhat smaller (5.4 ± 2.9 kJ mol^{-1}).
(23) Calculations for O_3, SO_2, and S_3 are discussed in: Jones, R. O. *Adv. Chem. Phys.* **1987**, *67*, 413.
(24) For a recent survey of this formalism and some of its applications, see: Jones, R. O.; Gunnarsson, O. *Rev. Mod. Phys.* **1989**, *61*, 689.
(25) Hohl, D.; Jones, R. O.; Car, R.; Parrinello, M. *Chem. Phys. Lett.* **1987**, *139*, 540.
(26) Hohl, D.; Jones, R. O.; Car, R.; Parrinello, M. *J. Chem. Phys.* **1988**, *89*, 6823.
(27) Car, R.; Parrinello, M. *Phys. Rev. Lett.* **1985**, *55*, 2471.
(28) Hohl, D.; Jones, R. O.; Car, R.; Parrinello, M. *J. Am. Chem. Soc.* **1989**, *111*, 825.
(29) Kohn, W.; Sham, L. J. *Phys. Rev.* **1965**, *140*, A1133.
(30) Vosko, S.; Wilk, L.; Nusair, M. *Can. J. Phys.* **1980**, *58*, 1200.
(31) Ceperley, D. M.; Alder, B. J. *Phys. Rev. Lett.* **1980**, *45*, 566.
(32) Bachelet, G. B.; Hamann, D. R.; Schlüter, M. *Phys. Rev. B* **1982**, *26*, 4199.

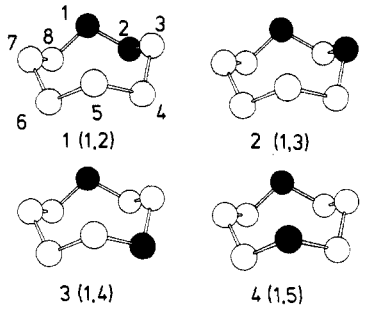

Figure 1. Structures of Se_2S_6 (and Se_6S_2).

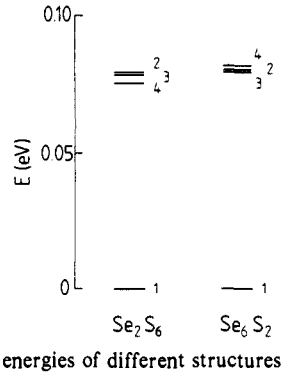

Figure 2. Relative energies of different structures in Se_2S_6 and Se_6S_2.

relative depths of local minima in the present work. The energy cutoff for the plane wave expansion of the eigenfunctions, ψ_i, was taken to be 144 eV (5.3 hartree au) corresponding to ~4000 plane waves. The convergence of geometries and relative energies with energy cutoff, number of k points, and the size of the unit cell has been studied in detail in our previous work on similar systems.[26]

An important advantage of the MD procedure is its ability to locate energy minima corresponding to geometries far removed from the initial structure. In each case we started with the ground-state geometry of S_8 (D_{4d}), with velocities $\dot{\psi}_i$ and $\dot{R}$ set equal to zero. The only explicit diagonalization in the calculation is performed for the initial geometry with a small plane wave basis set (energy cutoff 27.2 eV). The resulting eigenfunctions serve as initial input to iterative steepest descents methods, leading eventually to an accurate representation of ψ_i for this geometry (using the full plane wave basis). We then alternate steepest descents techniques ($\Delta t = 1.0 \times 10^{-15}$ s, $\mu_i = 50000$ au) with MD at $T = 200$ K ($\Delta t = 8.5 \times 10^{-17}$ s, $\mu_i = 300$ au) to locate the minimum and probe the local environment on the energy surface. Each structure determination required a total of about 4000 time steps, and the motion of the nuclei departs very little from the BO surface. The electronic system is kept within ~0.1 eV of its ground state, so that the molecular configurations observed represent physical entities at elevated temperatures.

In the simulated annealing runs, the average instantaneous temperature (T) (the mean kinetic energy of the ions) is kept constant with 10° tolerance by rescaling the ionic velocities uniformly with a factor $(\langle T \rangle / T)^{1/2}$. Within the framework of the LSD approximation and the basis described above, this approach allows us to determine the relative energies of the minima found to better than 1×10^{-3} eV. It is important to note, however, that there may be other local minima in the energy surface with similar structures and energies not accessible with the present annealing scheme and choice of temperatures, so that the optimum geometries and energies may be somewhat different. Each time step required approximately 1 s of CPU time on a Cray X-MP 416 computer.

III. Results for Se_xS_y

A. Se_2S_6, Se_6S_2. The cyclic structures possible in Se_2S_6 and Se_6S_2 are shown in Figure 1. The numeration of the atoms begins in each case on one of the minority atoms. The relative energies of the low-lying molecular states are shown in Figure 2, and the geometries corresponding to each structure are given in Tables I and II. The calculations make no assumptions about the symmetry of the molecules, and it can be seen that the departures from the symmetries given in the table are very small.

The structures show several remarkable features. In all eight structures, the three bond lengths (S–S, S–Se, Se–Se) are not only the same within 0.01 Å (2.08, 2.23, 2.35 Å) but also the S–S and Se–Se bonds are the same as found in our previous calculations for the ring structures of S_8 and Se_8. All three are simply the sums of the corresponding atomic radii. The idea of transferability between different structures is enhanced by the following observation. If we average the structural parameters, regardless of atom type, we find the same values in each of the four isomers of Se_2S_6 [$\langle d_{ij} \rangle = 2.15$ Å, $\langle \alpha_i \rangle = 108.0°$, $\langle \gamma \rangle = 98.7°$] and Se_6S_2 [$\langle d_{ij} \rangle = 2.29$ Å, $\langle \alpha_i \rangle = 107.4°$, $\langle \gamma \rangle = 99.5°$ in Se_6S_2]. If these averages are extrapolated to Se_0S_8 and Se_8S_0, we obtain structures close to the known structures of S_8 and Se_8.

The deviations found from the average values of the structural parameters are also quite regular. Replacing S by Se leads to the increased bond length expected from the atomic radii and locally to a reduction in both bond and dihedral angles. While the angle changes that result from changing a single atom type are not as localized as changes in the bond length, the perturbations

Table I. Molecular Parameters d, α, and γ for All Isomers of Se_2S_6 (see Figure 1)[a]

	(1,2)[C_2]	(1,3)[C_s]	(1,4)[C_2]	(1,5)[C_{2v}]
d_{12}	2.34	2.22	2.22	2.23
d_{23}	2.23	2.22	2.07	2.08
d_{34}	2.07	2.22	2.23	2.08
d_{45}	2.08	2.08	2.23	2.23
d_{56}	2.09	2.08	2.08	2.23
d_{67}	2.08	2.08	2.07	2.07
d_{78}	2.07	2.08	2.08	2.08
d_{81}	2.23	2.22	2.23	2.23
α_1	105.9	106.1	106.7	106.7
α_2	105.8	108.1	108.2	108.9
α_3	108.1	106.2	108.2	108.6
α_4	108.8	108.4	106.7	108.4
α_5	109.1	108.7	108.5	106.5
α_6	109.2	109.2	108.7	109.2
α_7	108.8	108.7	108.8	108.7
α_8	108.2	108.5	108.6	108.5
γ_{12}	96.8	98.0	98.3	99.1
γ_{23}	97.2	96.6	97.8	96.6
γ_{34}	97.6	96.1	96.3	98.2
γ_{45}	100.6	100.4	99.1	100.5
γ_{56}	102.9	102.1	101.1	99.0
γ_{67}	100.5	100.4	98.9	96.5
γ_{78}	97.5	99.0	99.1	97.7
γ_{81}	97.3	97.6	99.1	100.4

[a] Bond lengths d_{ij} (between atoms i and j) in Å, bond angles α_i (at atom i) and torsion angles γ_{ij} (at bond ij) in deg.

Table II. Molecular Parameters d, α, and γ for All Isomers of Se_6S_2 (see Figure 1)[a]

	(1,2)[C_2]	(1,3)[C_s]	(1,4)[C_2]	(1,5)[C_{2v}]
d_{12}	2.07	2.22	2.23	2.23
d_{23}	2.23	2.22	2.34	2.35
d_{34}	2.35	2.23	2.23	2.35
d_{45}	2.35	2.34	2.22	2.22
d_{56}	2.35	2.35	2.35	2.23
d_{67}	2.35	2.35	2.35	2.35
d_{78}	2.35	2.35	2.35	2.35
d_{81}	2.23	2.23	2.22	2.22
α_1	109.3	109.2	108.9	109.1
α_2	109.3	107.4	107.2	107.2
α_3	107.0	109.1	107.0	106.6
α_4	106.9	107.1	109.0	107.0
α_5	106.3	106.6	106.9	109.1
α_6	106.4	106.4	106.8	107.3
α_7	106.8	106.5	106.5	106.6
α_8	107.1	106.8	106.8	106.9
γ_{12}	101.9	100.9	100.6	97.8
γ_{23}	100.9	100.8	100.4	100.2
γ_{34}	99.8	100.4	100.9	101.1
γ_{45}	98.2	98.0	98.6	98.4
γ_{56}	96.3	98.5	98.1	97.6
γ_{67}	98.2	98.6	100.2	100.1
γ_{78}	99.8	98.2	98.4	101.1
γ_{81}	100.9	100.4	98.6	98.5

[a] Bond lengths d_{ij} (between atoms i and j) in Å, bond angles α_i (at atom i), and torsion angles γ_{ij} (at bond ij) in deg.

Table III. Molecular Parameters d, α, and γ for All Isomers of Se_2S_5 (see Figure 3)[a]

	1 (1,2)	**2** (2,3)	**3** (3,4)	**4** (4,5)	**5** (1,3)	**6** (2,4)	**7** (3,5)	**8** (2,7)	**9** (1,4)	**10** (2,5)	**11** (3,6)	**12** (2,6)
d_{12}	2.33	2.23	2.07	2.07	2.21	2.22	2.07	2.21	2.21	2.22	2.06	2.21
d_{23}	2.30	2.39	2.29	2.13	2.28	2.28	2.28	2.30	2.13	2.29	2.29	2.30
d_{34}	1.99	2.15	2.26	2.15	2.14	2.15	2.14	1.99	2.15	1.99	2.14	1.99
d_{45}	2.24	2.22	2.38	2.50	2.23	2.38	2.37	2.24	2.38	2.38	2.22	2.23
d_{56}	1.99	1.99	1.99	2.15	1.99	1.99	2.15	1.99	1.99	2.15	2.14	2.14
d_{67}	2.14	2.16	2.16	2.13	2.15	2.15	2.14	2.30	2.14	2.14	2.29	2.29
d_{71}	2.21	2.05	2.06	2.07	2.20	2.06	2.06	2.21	2.21	2.06	2.06	2.06
α_1	98.7	98.9	102.0	102.5	102.5	99.0	102.5	99.5	101.6	99.3	102.6	99.4
α_2	107.3	103.1	104.7	106.6	104.0	107.3	104.0	107.5	106.9	107.2	104.0	107.6
α_3	106.3	107.0	102.8	103.1	106.9	102.4	106.8	106.4	102.8	106.1	107.9	107.3
α_4	106.5	108.0	106.6	103.1	107.5	106.5	103.6	106.4	106.4	103.0	107.9	107.0
α_5	107.3	107.3	107.1	106.6	107.1	107.0	107.1	107.5	106.9	107.0	104.0	104.2
α_6	101.8	103.3	102.5	102.5	101.9	102.8	102.4	99.6	101.8	102.6	102.6	102.9
α_7	102.9	106.8	107.2	107.2	103.0	106.6	107.2	106.7	102.8	106.7	107.5	107.0
γ_{12}	71.4	74.5	75.5	75.9	73.7	73.0	76.3	73.0	74.1	73.2	77.0	73.6
γ_{23}	108.2	103.3	105.1	110.9	105.3	106.8	107.0	108.4	110.4	109.1	106.1	108.1
γ_{34}	86.6	83.8	82.8	84.0	84.9	84.8	82.8	87.1	85.9	85.0	82.5	84.4
γ_{45}	0.3	2.4	2.5	0.0	4.0	0.3	2.9	0.1	0.1	0.1	0.1	3.4
γ_{56}	88.1	85.5	84.5	84.0	85.2	86.5	83.8	87.2	85.9	86.2	82.6	85.2
γ_{67}	112.2	110.8	113.8	110.9	112.6	113.5	110.7	108.3	113.1	110.9	106.0	106.2
γ_{71}	74.4	76.4	77.0	75.9	74.6	76.3	76.7	73.0	74.4	76.0	76.9	76.1

[a] Bond Lengths d_{ij} (between atoms i and j) in Å, bond angles α_i (at atom i) and torsion angles γ_{ij} (at bond ij) in deg. Structures **4**, **8**, and **11** have a single mirror plane [C_s symmetry], the remainder have C_1 symmetry.

Table IV. Molecular Parameters d, α, and γ for All Isomers of Se_5S_2 (see Figure 3)[a]

	1 (1,2)	**2** (2,3)	**3** (3,4)	**4** (4,5)	**5** (1,3)	**6** (2,4)	**7** (3,5)	**8** (2,7)	**9** (1,4)	**10** (2,5)	**11** (3,6)	**12** (2,6)
d_{12}	2.05	2.21	2.33	2.33	2.21	2.21	2.33	2.21	2.22	2.21	2.33	2.22
d_{23}	2.29	2.13	2.29	2.40	2.28	2.28	2.29	2.29	2.40	2.28	2.28	2.27
d_{34}	2.27	2.15	1.99	2.14	2.15	2.14	2.14	2.27	2.16	2.26	2.15	2.27
d_{45}	2.50	2.49	2.38	2.22	2.49	2.37	2.38	2.52	2.36	2.37	2.50	2.51
d_{56}	2.28	2.28	2.27	2.14	2.28	2.26	2.14	2.27	2.28	2.14	2.15	2.15
d_{67}	2.40	2.40	2.40	2.40	2.39	2.40	2.40	2.29	2.40	2.39	2.28	2.28
d_{71}	2.23	2.34	2.34	2.33	2.22	2.33	2.34	2.21	2.22	2.33	2.33	2.33
α_1	103.3	103.1	100.6	99.5	100.9	103.3	100.1	102.4	101.5	101.3	99.7	102.1
α_2	104.9	107.5	107.4	104.3	107.2	105.0	107.2	105.0	105.7	105.0	107.2	105.3
α_3	104.6	104.9	107.6	108.4	104.2	108.2	103.9	103.6	108.8	104.8	103.9	104.7
α_4	103.7	103.9	104.0	108.4	103.9	104.4	108.0	103.7	105.8	107.1	103.9	103.2
α_5	104.2	103.1	104.1	104.2	104.0	104.0	105.5	104.9	106.8	103.5	107.2	105.5
α_6	100.2	99.8	99.1	99.5	100.0	99.9	99.7	102.4	100.0	99.9	99.7	100.6
α_7	107.9	104.3	104.1	103.3	107.7	104.2	103.9	103.8	108.3	103.9	103.9	105.4
γ_{12}	77.4	75.6	74.3	76.1	75.1	76.3	74.0	76.0	76.1	77.0	74.2	74.1
γ_{23}	111.1	114.3	113.2	108.4	112.0	111.4	111.7	112.3	105.9	110.8	112.4	109.4
γ_{34}	84.9	87.4	87.6	86.3	86.5	85.7	89.8	84.8	86.6	85.7	87.6	85.9
γ_{45}	0.2	2.7	1.9	0.1	2.1	0.3	0.8	0.0	4.5	1.5	0.1	0.4
γ_{56}	83.8	84.6	86.8	86.3	85.6	85.0	84.0	84.9	80.8	85.7	87.6	87.2
γ_{67}	108.6	108.5	107.6	108.3	108.4	107.7	108.8	112.3	106.5	109.8	112.5	113.0
γ_{71}	75.8	74.3	74.6	76.1	75.5	74.3	74.9	76.0	77.1	75.8	74.2	73.7

[a] Bond lengths d_{ij} (between atoms i and j) in Å, bond angles α_i (at atom i) and torsion angles γ_{ij} (at bond ij) in deg. Structures **4**, **8**, and **11** have a single mirror plane [C_s symmetry], the remainder have C_1 symmetry.

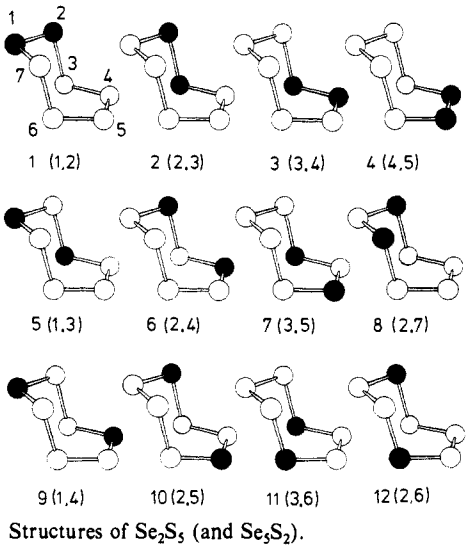

Figure 3. Structures of Se_2S_5 (and Se_5S_2).

are only of the order of 2°, so that the basic structures are very similar.

The relative energies shown in Figure 2 show that the (1,2)-structures are the ground states in both Se_2S_6 and Se_6S_2. The energies of the other structures are degenerate to within 3 meV and lie 0.08 eV above the ground state in each case. A simple model that explains these features of the energetics is discussed in detail in section IV. We note here that the (1,2)-isomer is the most prominent one detected in the NMR spectra of Se_2S_6 (there are smaller amounts of the other three) and the only one found in NMR spectra of Se_6S_2.[16]

B. Se_2S_5, Se_5S_2. The twelve different cyclic trans structures of Se_2S_5 and Se_5S_2 are shown in Figure 3. Structures **4**, **8**, and **11** have a single mirror plane (C_s symmetry), while there are no symmetry elements (other than the identity) in the other structures. The lower symmetries reflect the fact that the C_s chair structure of S_7 has less symmetry than the crownlike D_{4d} structure of Se_8 and S_8, the basis for the structures in the preceding section.

The structural parameters are given in Tables III and IV. They reflect well-established trends in cyclic group VIA molecules,[2,19,26]

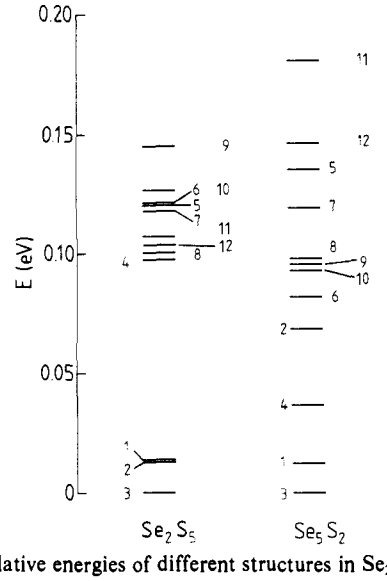

Figure 4. Relative energies of different structures in Se_2S_5 and Se_5S_2.

including the relationship between the bond length and dihedral angle, γ (the shortest bonds have γ values near 90° due to minimal lone-pair repulsion between neighboring atoms), and the fact that long bonds are adjacent to short bonds. The bonds 1–2, 2–3, 3–4, 4–5 are not related by symmetry in any of these clusters, and the ranges of bond lengths (1.99 to 2.50 Å) and dihedral angles are much greater than in the eight-membered rings. Within each bond type, however, we find the same transferability as noted above. The average 1–2 and 7–1 bond lengths, for example, are 2.06, 2.21, and 2.33 Å for S–S, S–Se, and Se–Se, respectively. As in the eight-membered rings, the replacement of S by Se leads to longer bonds and smaller bond angles.

The relative energies of the different structures are shown in Figure 4. The results are similar to those in Se_2S_6 and Se_6S_2 in that the structures with lowest energies have adjacent minority atoms. However, there is no evidence of systematic degeneracies, and the energy spread is larger in Se_5S_2 than in Se_2S_5. Our calculations have been restricted to the vicinity of the cyclic trans (or "chair") structures derived from the ground-state structure of S_7 or Se_7. Our previous calculations[25,26] indicate, however, that the cis or "boat" structures of the homocyclic molecules lie only ~0.1 eV higher. We therefore expect that heterocyclic structures derived from the latter will also lead to a band of total energies similar to those for the trans form, so that the final spectrum for each molecule will be very complicated. While structures with neighboring minority atoms are the best candidates for the states with lowest energy, the precise ordering of the remainder within the bands is difficult to predict. This ordering may also be irrelevant, as many structures are likely to coexist in any given system.

C. Dynamics in Se_2S_5. Chemists often view mixtures of different molecules in solution and in the liquid phase (whether isomers or conformers) as comprising molecules that are essentially static: apart from vibrations around the equilibrium geometry, the individual molecules are not seen as dynamically changing entities. This view is fostered by numerous theoretical calculations aimed at finding symmetric structures at $T = 0$ and their characteristic vibrational modes. However, solutions and liquids are usually kept at higher temperatures (often $T = 300$ K) and other dynamic phenomena could influence the structure of the constituent molecules. An example is the spectroscopic evidence in Se_2S_5 at room temperature[17] for dynamical structural changes ("pseudorotation") between different (1,2)-conformers [labeled **1** to **4** in Figure 3]. To study the dynamical properties of this molecule, we have coupled it to a heat bath of $T = 300$ K, simulating the interaction with the environment by a rescaling of the atomic velocities.[33]

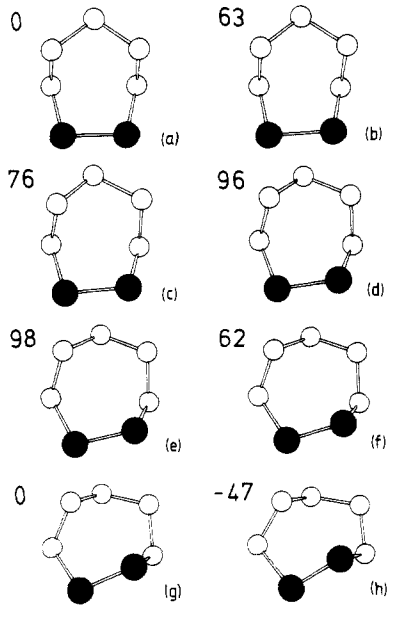

Figure 5. Molecular dynamics of Se_2S_5 at $T = 300$ K, showing the change from the (4,5)-structure (a) to the ground-state (3,4)-structure (h). The interval between each plot is $500\Delta t$, with $\Delta t = 8.5 \times 10^{-17}$ s. The energies relative to the starting energy are shown in meV.

We began with the (4,5)-structure (**4** in Figure 3), which has the highest energy of the structures with neighboring Se–Se atoms. After finding the C_s structure with energy shown in Figure 4, we continued the molecular dynamics at a temperature of 300 K and show the geometry changes occurring in the first 3.0×10^{-13} s (3500 times steps, $\Delta t = 8.5 \times 10^{-17}$ s) in Figure 5. The energy increases to a value 0.12 eV above the starting energy. This is an upper bound to the potential energy barrier between the two structures, and the corresponding geometry is close to the one shown in Figure 5e. After crossing this barrier, the molecule has a structure with the same pattern of torsion angles ("motif")[34] as the ground state, and the energy falls rapidly to a local minimum corresponding to the geometry shown in Figure 5h. If we now use the above procedure to locate the related minimum of the potential energy surface (at $T = 0$), we find the ground-state energy and structure (Table III) with the accuracy quoted above (better than 10^{-3} eV). This is a severe test of the calculation, since the orientations of the molecule in the unit cell are quite different. The energy is 0.22 eV (20 kJ mol^{-1}) below the top of the barrier, similar to the value of the torsion barrier quoted above for S_7.[19]

A comparison of the (4,5)- and (3,4)-structures (Table III) shows that the geometry changes are substantial. The Se–Se bond length changes from 2.50 to 2.26 Å, and the dihedral angle from zero to 82.8°. In fact, the bond length *increases* to 2.52 Å before decreasing to its final value. The bond angle changes are much smaller. Figure 5 shows that the change in structure involves a concerted change of the positions of all atoms, with the largest motion apparent in the Se atom 4. During this simulation, the maximum instantaneous temperature fluctuations ($\langle T - \langle T \rangle \rangle$ for the individual atoms were found to be as high as 750°, i.e. the kinetic energy distribution over the atoms is far from uniform. At any instant in time, individual atoms can have a kinetic energy of ~0.1 eV, sufficient to surmount energy barriers such as the structural change **4** → **3**.

In order to study the dynamics further, we performed an extended simulation of 60000 time steps from the ground-state structure (**3**) in Figure 3. The structural changes were substantial, with the highest energy being ~0.12 eV above the ground-state energy. This was insufficient, however, for the system to cross a barrier to one of the other stable local minima depicted in Figure 3. The system remained in the basin of attraction[35] of the

(33) Woodcock, L. V. *Chem. Phys. Lett.* **1971**, *10*, 257.

(34) Tuinstra, F. *Structural Aspects of the Allotropy of Sulphur and Other Divalent Elements*; Waltman: Delft, 1967.

ground-state structure throughout, and this was also true in a second simulation we performed at 500 K (10000 time steps) starting from the structure and velocities found at the top of the energy barrier between structures **4** and **3**.

These results suggest that in solutions or in the liquid phase statistical averages over structurally different molecules dominate the properties in question. The individual constituents can change their shapes constantly as dictated by the temperature of the bath and the shape of the energy surface. In the seven-membered rings basins of attraction (local minima) of different extent are separated by barriers that can be overcome at $T = 300$ K. While the time required for the conversion **4** → **3** in Se_2S_5 (4×10^{-13} s) is much shorter than the NMR time scale, our maximum simulation period (5 ps) was not long enough to observe further structural changes. The basin of attraction for the ground state **3** is not only deeper by ≥0.05 eV, but it is apparently more extended.

IV. Model Description of Energy Differences in Se_xS_y Rings

The calculations presented in the previous section show some remarkable regularities, particularly in predicting ground states with adjacent minority atoms in each case. We now show that the binding trends can be understood in terms of a very simple model.

A. Se_2S_6, Se_6S_2. The eight-membered rings are characterized by small deviations from the crown-shaped [D_{4d}] structures familiar from S_8 and Se_8. We have also seen that there are three bond lengths in the clusters, $d_{S\text{-}S}$, $d_{S\text{-}Se}$, and $d_{Se\text{-}Se}$. The well-known relationship between bond length and bond strength[36] suggests that we associate with each bond type in these cyclic molecules corresponding contributions to the binding energy, $E_{S\text{-}S}$, $E_{S\text{-}Se}$, and $E_{Se\text{-}Se}$. In the case of the 1–2 structure in Se_2S_6, this leads to

$$E_{1\text{-}2} = E_{Se\text{-}Se} + 2E_{S\text{-}Se} + 5E_{S\text{-}S} \quad (5)$$

For *all three* remaining structures, we find

$$E_{1\text{-}3,1\text{-}4,1\text{-}5} = 4E_{S\text{-}Se} + 4E_{S\text{-}S} \quad (6)$$

From this simple argument we may then expect the energies of three structures to be equal, and the fourth ($E_{1\text{-}2}$) to differ by the amount

$$\Delta E = E_{Se\text{-}Se} + E_{S\text{-}S} - 2E_{S\text{-}Se} \quad (7)$$

If we apply the same argument to the Se_6S_2 structures, eq 5 and 6 still apply, with S and Se interchanged. Again we find the (1–2) structure separated from the other three, and the energy difference is precisely that given in eq 7. This very simple argument explains why the energy orderings in Se_2S_6 and Se_6S_2 are the same and is consistent with the (1–2) ground states being separated from three structures with almost equal energies. The separation in the present calculations is approximately 0.08 eV (7.4 kJ mol^{-1}), which is consistent with the endothermicity of reaction 2 and in reasonable agreement with the measured heats of reaction in the gas and liquid phases.

B. Se_2S_5, Se_5S_2. The structures of the seven-atom rings have little or no symmetry, with a larger range of bond lengths than in the eight-membered rings. However, the bond angles lie in a rather narrow range (99–109°) and we have seen that the bond lengths are transferable within bond type (given by its position 1–2, 2–3, 3–4, or 4–5 in the ring). If we apply the approach of the preceding section to a seven-membered ring with equal bond lengths, we again find a structure with adjacent minority atoms separated from two other states by ΔE. Since the basic C_s structure of S_7 or Se_7 has four inequivalent bonds, we may then expect the energies in Se_2S_5 or Se_5S_2 to comprise two groups, one with the four structures with adjacent minority atoms and a second with the eight others.

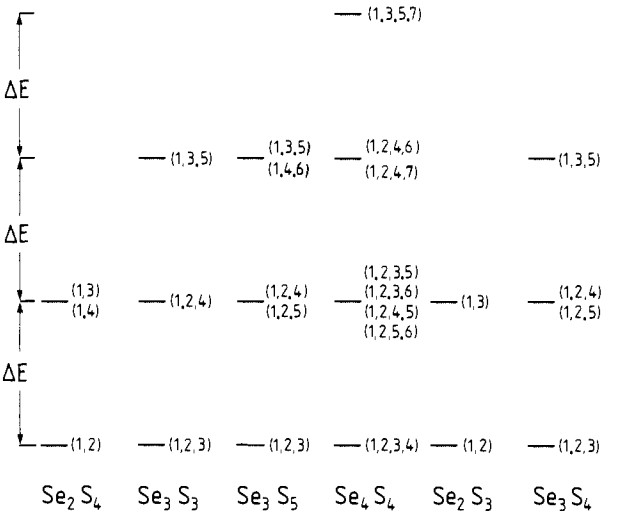

Figure 6. Predictions of simple model for relative energies in Se_xS_y heterocycles. ΔE is the energy difference defined in eq 6.

These features are apparent in the results of Figure 4, where the low-lying states in both Se_2S_5 and Se_5S_2 all correspond to structures with adjacent minority atoms. It is not surprising that such a simple model cannot describe the precise ordering of the energies, but the trends are satisfactory. If one calculates the mean energies of the two groups of levels, the separations in Se_2S_5 (0.073 eV) and Se_5S_2 (0.087 eV) are in reasonable agreement with each other and with the value found in the eight-membered rings (0.082 eV).

C. Predictions for Other Cyclic Molecules Se_xS_y. The above arguments make the results of the calculations extremely plausible, and it is tempting to apply them to other heterocyclic molecules of the same type. We have seen that transferability of the three kinds of bonds (S–S, S–Se, Se–Se) results in simple expressions for the energy differences between the different structures, and the same assumptions applied to other systems result in the energies shown in Figure 6. Our experience has shown that the arguments apply best to symmetric structures arising in rings with an even number of atoms, and we discuss separately (a) Se_2S_4, Se_3S_3, Se_3S_5, Se_4S_4 and (b) Se_2S_3 and Se_3S_4. Identical arguments apply to the complementary structures, i.e. the model predicts the same energy ordering for Se_3S_5 and Se_5S_3.

The six- and eight-membered rings should have structures that are derived from those of S_6 and S_8, where all bond lengths are the same. The model predicts a series of levels separated by the energy difference ΔE (see eq 6). The ground state in each case corresponds to the structure with the most homonuclear bonds between minority atoms, and the ordering of the levels correlates directly with that number. In Se_4S_4, for example, the structures (in decreasing order of stability) correspond to three, two, one, and zero S–S bonds. In this case, we find the most structures (8), the greatest range of energies ($3\Delta E$), and the greatest degeneracy (4). The four structures found in the NMR work of Laitinen and Pakkanen[16] all belong to the two lowest levels. The single state identified in NMR spectroscopy of Se_5S_3 is the ground state anticipated by our model, and the three states found in Se_3S_5 are also the lowest lying (see Figure 6).

Five- and seven-membered rings are derived from the C_s structures of S_5 and S_7. There are three inequivalent bonds in the former and four in the latter, so that the single energies show in Figure 6 will split into groups. In Se_2S_3 (and Se_3S_2) we expect the three structures with neighboring minority atoms [(1,2), (2,3), (3,4)] to be the lowest lying, with a second group of three where the minority atoms are separated by a majority atom [(1,3), (2,4), (5,2)]. There are 16 inequivalent ways of distributing three minority atoms in the trans structures of Se_3S_4, with the same number of cis (boat) structures. For each type, our arguments indicate that the lowest lying structures will be those with the most

(35) This is referred to as the "catchment region" by: Mezey, P. G. *Int. J. Quantum Chem. Symp.* **1984**, *18*, 675. For a further discussion and references concerning potential energy surfaces, see: Mezey, P. G. *Potential Energy Hypersurfaces*; Elsevier: Amsterdam, 1987.

(36) For a discussion of the relationship between core size, valence eigenfunctions and bond strengths, see: Harris, J.; Jones, R. O. *Phys. Rev. A* **1979**, *19*, 1813.

Se–Se bonds, a group of eight will lie above them, and still higher will be the four structures where there are no homonuclear bonds between minority atoms. Our experience with Se_2S_5 and Se_5S_2 suggests that the groups of levels could overlap.

The parameter ΔE defined in eq 6 plays a central role in the present arguments. The energy difference refers, of course, to the ring structures and our calculated value ($\sim$0.08 eV) could differ from the corresponding values for the liquid and for the diatomic molecules. We noted above that the last two values indicated that reaction 1 is endothermic, in agreement with the ordering of levels we obtain. We have been somewhat fortunate to choose a system for which ΔE is sufficiently large that we could determine the trends in the stabilities of the different structures. By contrast, Drowart and Smoes[22] have shown that both the enthalpy and the difference in dissociation energies of the reaction

$$Se_2 + Te_2 \rightarrow 2SeTe \quad (8)$$

are zero to within the experimental uncertainty. In liquid mixtures of Se and Te, entropy effects are important and the enthalpy of mixing is *negative* throughout the composition range.[21] Predictions based on simple arguments must then be treated with caution in cases such as the Se–Te bond. It is nevertheless interesting to note that the difference in the dissociation energies of the reaction

$$S_2 + O_2 \rightarrow 2SO \quad (9)$$

has the opposite sign to reaction 1, with SO being the most stable of the three molecules. The special status of first-row atoms is well-known[36] and we have noted elsewhere the unusual behavior of oxygen in its inability to form bridge bonds (–S–O–S–) with sulfur.[28]

V. Concluding Remarks

We have described here calculations of the energy surfaces of all cyclic isomers of Se_2S_6 and Se_6S_2 and the trans isomers of Se_2S_5 and Se_5S_2. We have used an MD–DF method that requires no assumptions about the equilibrium structure. This is an important advantage in clusters of this size, where the energy surfaces are very complex, the structures have low symmetry, and there are numerous local minima. The focus on very small energy differences means that the energy minimization must be performed with care. The most stable structures in all molecules have adjacent minority atoms, and an extended simulation at 300 K (60000 time steps, 5 ps) for Se_2S_5 found one change between neighboring structures of this type. There are large variations in the instantaneous energy contributions of the individual atoms, so that energy barriers of the order of 0.1 eV can be overcome even at room temperature.

The unexpected simplicity of the results for the eight-membered rings and the transferability of bond parameters between different structures have suggested a simple model for predicting the stable structures of other cyclic Se_xS_y molecules. The results are in good agreement with trends found in recent measurements using Raman and NMR spectroscopies, in particular with the relative abundance of structures with adjacent minority atoms. The symmetry between the energy ordering of the isomers of Se-rich and S-rich molecules is in direct contrast to earlier discussions of these systems.[4,10] This symmetry is perturbed, of course, by differences between the elements such as atomic radius, but the essential features are not changed. The trend to "segregation" of minority components could also occur in the disordered liquid and amorphous states.

The combination of molecular dynamics and density functional methods has given useful results in S_7O, where the geometry changes and the energy barrier between the ring and ground-state structures are both very large. In the present work we have studied the opposite extreme—structures with very small energy differences and energy barriers that are small on a thermal scale. While no method can guarantee finding the absolute energy minima in the low-symmetry clusters of this size, the results demonstrate further the value of this approach.

Acknowledgment. We thank R. Steudel for discussions and for suggesting a study of Se_xS_y molecules, J. Heinen for developing the graphics software used to visualize the results, and K. Hilpert for useful remarks on high-temperature mass spectroscopy. We also thank the German Supercomputer Centre (Höchstleistungsrechenzentrum, HLRZ) for a generous grant of computer time on the Cray X-MP 416 in the Forschungszentrum Jülich.